# Drivers of Dry Day Sensitivity to Increased CO2

H. Douville, R. Chadwick, M. Saint-Lu, B. Medeiros

AGU ADVANCING EARTH AND SPACE SCIENCES

Geophysical Research Letters®

RESEARCH LETTER
10.1029/2023GL103200

# Drivers of Dry Day Sensitivity to Increased $CO_2$

**H. Douville[1], R. Chadwick[2,3], M. Saint-Lu[4], and B. Medeiros[5]**

[1]Centre National de Recherches Météorologiques, Université de Toulouse, Météo-France, CNRS, Toulouse, France, [2]Met Office Hadley Centre, Exeter, UK, [3]Department of Mathematics, Global Systems Institute, University of Exeter, Exeter, UK, [4]Laboratoire de Météorologie Dynamique (LMD), Institut Pierre Simon Laplace (IPSL), Sorbonne Université, CNRS, École Normale Supérieure, École Polytechnique, Paris, France, [5]National Center for Atmospheric Research, Boulder, CO, USA

**Key Points:**

- AGCM simulations are used to split the dry day response to increased $CO_2$ into fast adjustment versus slower uniform and patterned SST effects
- None of the three components consistently dominates the global land response of dry days across the selected CMIP6 models
- The uniform SST warming dominates the regional anomalies, which however do not scale with global warming across the multi-model ensemble

**Supporting Information:**

Supporting Information may be found in the online version of this article.

**Correspondence to:**

H. Douville,
herve.douville@meteo.fr

**Citation:**

Douville, H., Chadwick, R., Saint-Lu, M., & Medeiros, B. (2023). Drivers of dry day sensitivity to increased $CO_2$. *Geophysical Research Letters*, *50*, e2023GL103200. https://doi.org/10.1029/2023GL103200

Received 8 FEB 2023
Accepted 8 JUN 2023

**Author Contributions:**

**Conceptualization:** H. Douville
**Data curation:** H. Douville, R. Chadwick, M. Saint-Lu, B. Medeiros
**Formal analysis:** H. Douville, R. Chadwick, M. Saint-Lu
**Methodology:** H. Douville, R. Chadwick
**Supervision:** H. Douville
**Validation:** H. Douville
**Writing – original draft:** H. Douville, R. Chadwick, M. Saint-Lu, B. Medeiros



**Abstract** Persistent precipitation deficits are among the most impactful consequences of global warming. Here we focus on changes in the annual number of dry days (NDD) and in the annual maximum length of dry spells due to a quadrupling of atmospheric $CO_2$. We use atmosphere-only simulations to decompose the projected changes into additive contributions. A fast adjustment leads to a global increase in NDD despite notable regional exceptions (e.g., South Asia and Sahel). The effect of the uniform component of the surface ocean warming is model-dependent but shapes the regional distribution of the NDD response in each model. Finally, the ocean warming pattern also contributes to large uncertainties, likely through contrasting changes in large-scale circulation. Our results thus highlight the complexity of the NDD response, with policy-relevant practical implications for mitigation and adaptation strategies.

**Plain Language Summary** Global warming is expected to intensify the global water cycle, including the intensity and frequency of precipitation extremes. Yet, the response of the dry side of the daily precipitation distribution to increased atmospheric $CO_2$ has received so far less attention. Here we show that this response remains highly model-dependent across the latest generation of global climate models. Furthermore, we use atmosphere-only simulations to isolate different drivers of the precipitation response. A fast radiative and vegetation adjustment to increased $CO_2$ leads to an overall increase in the mean annual number of dry days (NDD) despite some regional exceptions. The effect of the ocean surface warming is highly model-dependent, only partly due to the diversity of the simulated patterns of sea surface temperature anomalies. The regional response of NDD and of the maximum length of dry spells thus does not simply scale with global warming across the different models.

## 1. Introduction

The latest generation of coupled ocean-atmosphere global climate models project a global increase in annual mean precipitation of 1%–3% for every 1°C of warming (Douville et al., 2021). This increase is determined by a robust response to global mean surface air temperature (2%–3% per 1°C) that is partly offset by fast adjustments to atmospheric radiative heating by greenhouse gases and aerosols (Allan et al., 2020; Fläschner et al., 2016). More intense but less frequent precipitation events have been observed across many regions (Donat et al., 2019; Giorgi et al., 2011), with projections of an increased incidence of extreme precipitation events coupled with longer dry spells (Sillmann et al., 2013; Thackeray et al., 2018). Yet the projections of regional precipitation remain highly uncertain, and their total variance is still dominated by model uncertainty rather than emission scenarios or internal climate variability (Douville et al., 2021; Lehner et al., 2020).

Beyond the fast adjustment due to its radiative effect, increased atmospheric carbon dioxide ($CO_2$) may also trigger a fast vegetation adjustment that is now accounted for in most Earth System Models. In response to high ambient $CO_2$ concentrations, many plants reduce their stomatal conductance and transpiration in order to minimize water loss, thereby increasing their plant water-use efficiency. This decrease in transpiration, however, may be partly offset by a $CO_2$ fertilization effect that favors photosynthesis and vegetation density. The net physiological $CO_2$ effect can affect the amount and variability of soil moisture and evapotranspiration, which in turn can influence the frequency, intensity, and duration of precipitation events. It may thus contribute to model uncertainty, especially in forested areas (Chadwick et al., 2017; Richardson et al., 2018; Skinner et al., 2017).

Projections of dry spells and meteorological droughts (Ukkola et al., 2020) have so far drawn less attention than projections of heavy precipitation, although they also have large potential impacts on land ecosystems and

human societies. One interesting exception is the CMIP5 multi-model study by Polade et al. (2014) highlighting the key role of dry days in changing regional climate and precipitation regimes under a high-emission RCP8.5 scenario. These results have been further supported by a CMIP6 single-model study (Douville & John, 2021) which examined experiments from the third phase of the Cloud Feedback Model Intercomparison: Project (Webb et al., 2017). A set of atmosphere-only (AGCM) experiments were used to decompose the AOGCM response to an idealized abrupt quadrupling of atmospheric $CO_2$ into separate contributions from uniform SST warming, the pattern of SST anomalies, as well as fast radiative and physiological $CO_2$ effects. In agreement with a previous pilot study (Chadwick et al., 2017), the balance between the different components varied strongly between different regions. The mean annual number of dry days (NDD) (hereafter NDD) and the annual maximum of consecutive dry days (MCDD) however showed a strong fast adjustment to increased $CO_2$.

As shown by Chadwick et al. (2017), such findings are model-dependent and deserve further investigation within CFMIP (Webb et al., 2017). The aim of the present study is to analyze changes in dry days/spells and their relationship with other precipitation responses in idealized abrupt-4x$CO_2$ experiments from a large set of CMIP6 models. A smaller subset of AGCM experiments is also explored in order to repeat the decomposition of the parent AOGCM response proposed by Chadwick et al. (2017) and Douville and John (2021). Although limited in number, this subset of four state-of-the-art models is shown to be representative of the overall CMIP6 response of daily precipitation.

## 2. Data and Methods

The piControl and abrupt-4x$CO_2$ experiments from a set of 32 CMIP6 models with daily precipitation outputs have been considered. In addition, some CFMIP-Tier-2 atmosphere-only simulations (c.f. Table S1 in Supporting Information S1) from a subset of 4 available AGCMs have been also analyzed. Their parent AOGCMs are a representative subset of CMIP6 models: CNRM-CM6-1 (Voldoire et al., 2019), IPSL-CM6A-LR (Boucher et al., 2020), HadGEM3-GC31-L (Williams et al., 2017), and CESM2 (Danabasoglu et al., 2020). Hereafter, they will be referred to as the names of the corresponding modeling center (c.f. Table S2 in Supporting Information S1). For each model, the abrupt-4x$CO_2$ experiment was started from the piControl experiment at year 0 and climate change was then diagnosed as the difference between the abrupt-4x$CO_2$ and piControl experiments from year 111–140. Before analysis, all model outputs have been regridded to a common medium-resolution (1.4°) horizontal grid derived from the CNRM-CM6-1 model.

All AGCM experiments are 30-year time-slice simulations after spin-up. The first pair, piSST and a4SSTice-4x$CO_2$, aims at replicating the piControl and abrupt-4x$CO_2$ coupled experiments. This is done by prescribing the same atmospheric $CO_2$ concentrations but also monthly mean annually varying oceanic boundary conditions derived from the SST and sea-ice concentration (SIC) simulated from year 111–140. It has been verified that, despite the lack of coupling, these AGCM experiments capture most regional details of the corresponding AOGCM response, for both annual mean precipitation (Figure S1 in Supporting Information S1) and the mean annual NDD (Figure S2 in Supporting Information S1). The other intermediate AGCM experiments allow us to decompose the total AGCM response (a4SSTice-4x$CO_2$ minus piSST) into three additive contributions (c.f. Table S3 in Supporting Information S1): a fast adjustment to increased $CO_2$ (a4SSTice-4x$CO_2$ minus a4SSTice), a model-dependent pattern of SST and SIC anomalies (a4SSTice minus piSST-pxK), and a model-dependent uniform SST warming (piSST-pxK minus piSST). Moreover, the fast adjustment to increased $CO_2$ can be also estimated from an AGCM simulation with preindustrial oceanic boundary conditions (piSST-4x$CO_2$) and has been thus further decomposed into a purely radiative $CO_2$ effect (piSST-4x$CO_2$-rad minus piSST) versus a physiological $CO_2$ effect obtained as a residual (piSST-4x$CO_2$ minus piSST-4x$CO_2$-rad). All anomalies or differences are estimated from pairs of 30-year simulations and their statistical significance are assessed using a two-sided *t*-test at the 5% level while adjusting the *p*-values for multiple testing (Wilks, 2016).

## 3. Results

Before analyzing changes in the NDD (below a 1 mm/day threshold) and their breakdown, Figure 1 shows how the annual mean precipitation response to an abrupt $CO_2$ quadrupling arises from two main contributions: changes in daily precipitation frequency and intensity. As explained in Douville and John (2021), this breakdown is only approximate since dry (wet) days are defined as days with intensity less (more) than 1 mm/day which also

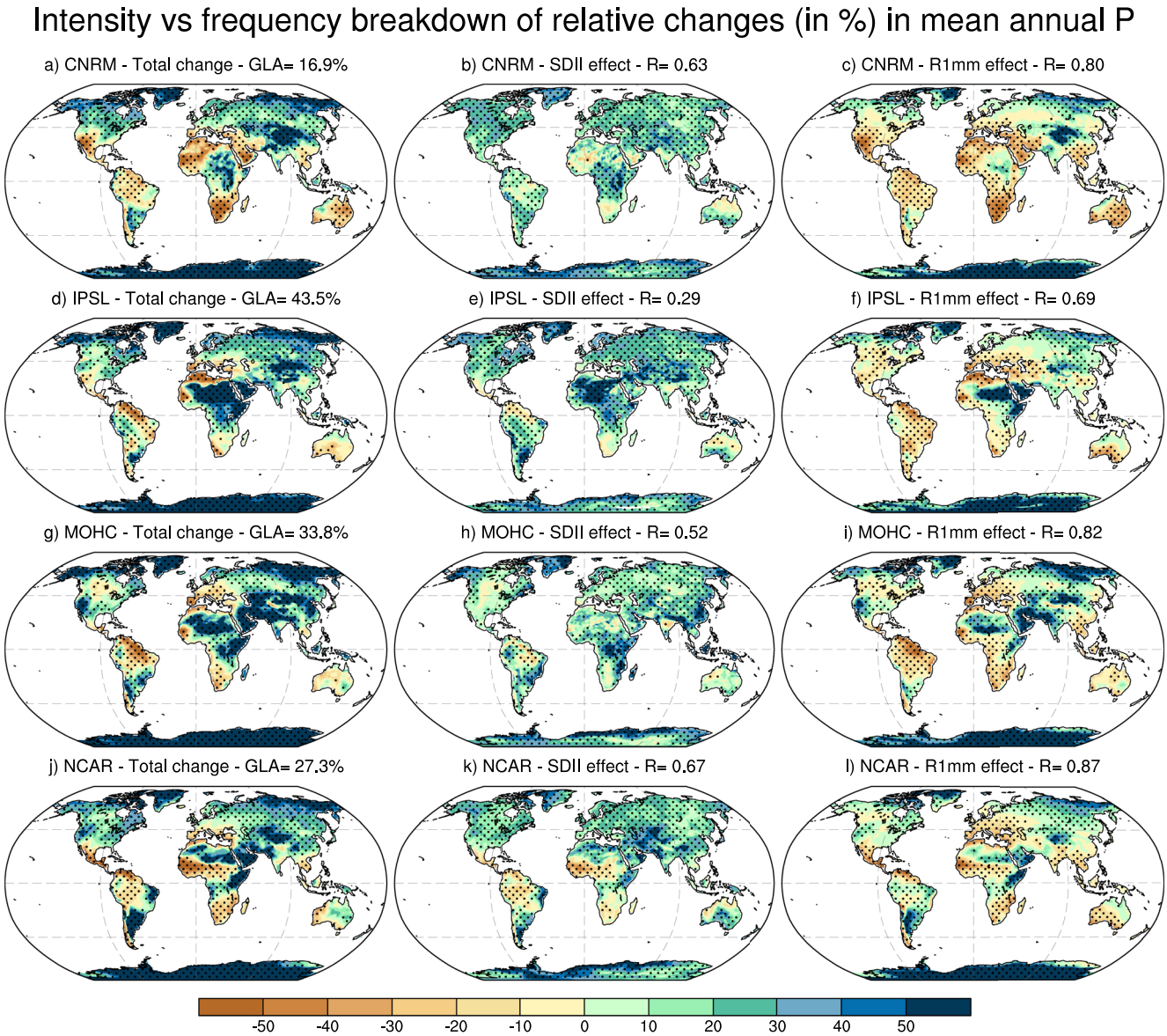


**Figure 1.** Breakdown of relative changes (%) in annual mean precipitation into intensity versus frequency components. The total changes (left panels) are split into two components (see text for details) for each of the four selected models (on each row): the contribution of relative changes in daily precipitation intensity (SDII effect, middle column) and the contribution of relative changes in daily precipitation frequency (R1mm effect, right column). Stippling highlights areas where changes are significant at the 10% level. In the left panels, global land average (GLA) denotes the GLA of the total relative changes. In other panels, *R* denotes the spatial anomaly correlation coefficient with the corresponding left panels.

contribute to the annual totals. In line with their preliminary results based on longer simulations with the CNRM AGCM, changes in daily mean precipitation intensity of wet days (SDII) lead to an overall increase in annual precipitation over land despite some regional exceptions. In the four models, these include Southern Africa and part of Australia and Amazonia. Yet, there are other regions with a poor model agreement, especially West Africa where the IPSL and NCAR models show opposite results. In contrast, changes in the wet day frequency (R1mm) lead to an overall decrease and a more spatially heterogeneous precipitation response.

In agreement with previous CMIP5 studies (e.g., Polade et al., 2017), all models project a strong drying around the Mediterranean as well as over most subtropical Mediterranean-like regional climates (e.g., Southern Africa, Australia, Chile), Amazonia and southeast Asia. Again, there are also regions with a poor model agreement, not only West Africa but also the western US for instance. Both SDII and R1mm changes contribute to the annual mean precipitation response. Yet, and as highlighted by Douville and John (2021), the spatial correlations with

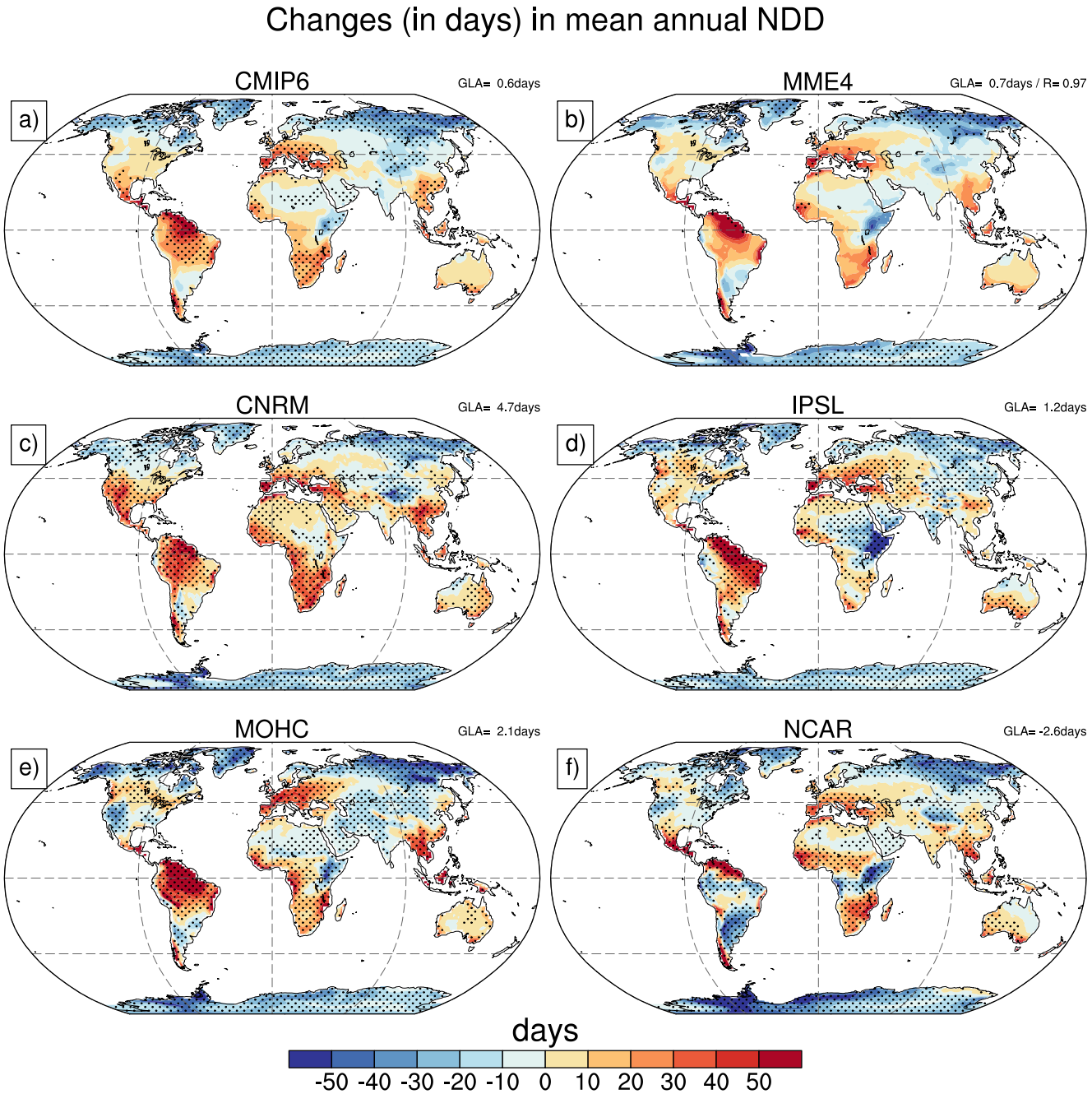


**Figure 2.** Changes in the mean annual number of dry days as simulated by (a) the full CMIP6 ensemble, (b) MME4, the selected subset of four models, (c) CNRM, (d) IPSL, (e) MOHC, and (f) NCAR. Stippling highlights areas where changes are significant at the 10% level and global land average (GLA) denotes the GLA of the simulated changes.

changes in SDII and R1mm respectively (*R* in the middle and right panels) denote that the global distribution of the precipitation response is mostly shaped by changes in the wet day frequency (and this would be even more the case if both land and sea were considered). Our results thus confirm that changes in daily precipitation intensity, while important for understanding the response of precipitation extremes (John et al., 2022), do not necessarily dominate the regional response of annual mean precipitation, so the NDD is also an important metric to analyze.

Figures 2a and 2b compare the ensemble mean response of the mean annual NDD between the full set (32) and the selected subset (only 4) of CMIP6 models. As claimed earlier, our subset is quite representative of the full ensemble with very similar spatial patterns (as revealed by the 0.97 pattern correlation between the full ensemble

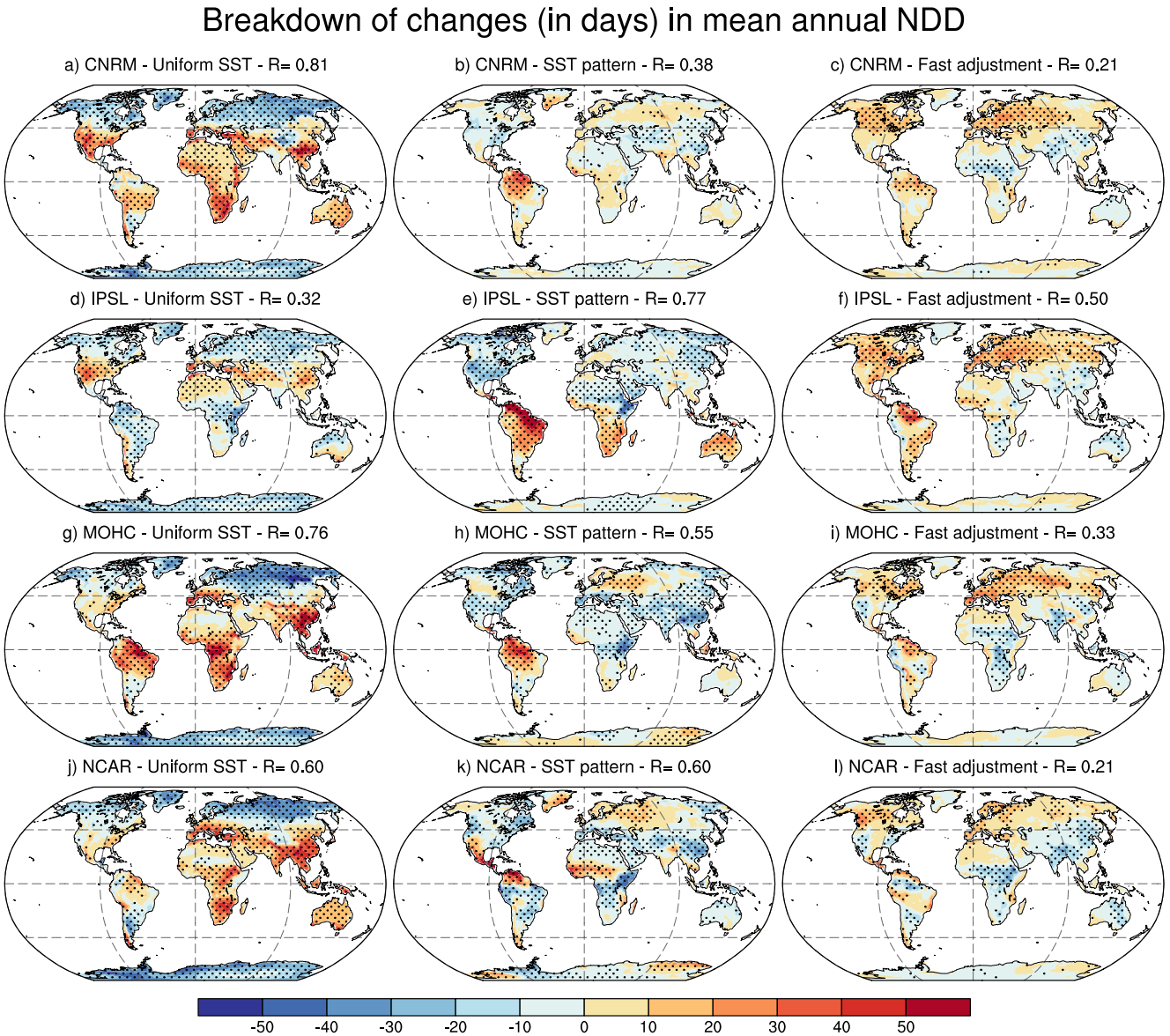


**Figure 3.** Breakdown of changes in the mean annual number of dry days. The total changes are split into three contributions for each of the four selected models: the response to the uniform component of SST warming (left panels), the response to the geographical pattern of the SST change (also including changes in sea-ice cover, middle column), and the fast adjustment to increased $CO_2$ levels (right panels, this fast $CO_2$ effect is further split into radiative vs. physiological effects in Figure S3 in Supporting Information S1). Stippling highlights areas where the difference is significant at the 10% level and *R* denotes the spatial anomaly correlation coefficient with the total AGCM response shown in Figure S2 in Supporting Information S1.

mean and sub-ensemble mean) showing a substantial increase of NDD over Amazonia, Mexico, southern Europe, southeast Asia, South Africa, southern Australia, and Chile. This widespread drying leads to a positive global land average change despite some significant regional decreases, especially in the northern high-latitudes. Beyond this apparent multi-model agreement, there is also a substantial inter-model spread as revealed by Figures 2c–2f showing the individual responses of the 4 selected CMIP6 models. Contrasted regional responses are found for instance over the western US and part of South America, but the spread can be also strong in drying areas where the models agree about the sign of the anomalies but not about their magnitude (e.g., Southern Africa).

What then may explain these significant disparities across the CMIP6 models? Our CFMIP experiments allow us to compare different potential drivers for the selected subset of four models (Figure 3). Note that we only show here the AGCM breakdown since the total AGCM response has already been shown to capture that of the corresponding CMIP6 models (Figure S2 in Supporting Information S1). The first considered contribution

(left panels) arises from the uniform SST warming which was prescribed from the individual CMIP6 models and therefore differs slightly across our four models (although they are all in the upper range of the equilibrium climate sensitivity). In all of them, this uniform component of the global ocean warming leads to a widespread drying (except in the northern high-latitudes) that strongly contributes to the total NDD response (as revealed by the correlation with the corresponding geographical patterns found over land). The IPSL model, however, shows less consistent changes than the other three models, with many regions showing a wetting response, as well as a lower correlation ($R = 0.38$) with the total response. In contrast, it shows a dominant contribution of the SST warming pattern effect (middle column, $R = 0.67$), thereby suggesting a key role of large-scale circulation anomalies potentially driven by such spatial gradients in four times $CO_2$ SST anomalies. This contribution is also large in the other models, especially in the tropics where the sign of the anomalies differs between different regions and models. Finally, the last contribution (right panels) from the fast adjustment is reasonably robust across the four models, with mostly positive anomalies in the northern extratropics and negative anomalies over the African and South Asian monsoon regions.

While this contribution does not dominate the overall pattern of the total response over land, it plays a key role in some densely vegetated regions thereby suggesting a possible role for the physiological effect. Reduced plant transpiration generally makes rainfall less frequent (Figure S3 in Supporting Information S1). Over Amazonia in particular, the physiological effect strongly contributes to the total NDD increase. This is less clear over the rainforest of central Africa, where the radiative effect of increased $CO_2$ overcomes the physiological effect and tends to decrease NDD. The balance between the two effects is a source of model disagreement for the total NDD response, especially over central Africa.

Looking now at changes in the annual maximum length of consecutive dry days over land (MCDD, Figure S4 in Supporting Information S1), the spatial pattern is very varied, resembling to a certain extent both the patterns of mean precipitation change (Figure 1) and the change in NDD (Figure 2). In particular, there is a consistent increase in MCDD in most subtropical regions, including the Mediterranean basin itself but also California, Chile, Southern Africa, and Australia. Changes in MCDD and NDD are likely to be closely related, though MCDD is more directly linked to changes in dry season length in all tropical and subtropical regions with an absolutely dry season in which no significant precipitation event (above 1 mm/day) can occur. The dry season length is projected to expand over Amazonia and Southeast Asia, with potential impacts on widespread rain-forests. Note however that MCDD is computed based on consecutive dry days during the calendar year, and thus does not account for the full dry season in the northern tropics where it generally overlaps two consecutive years.

When broken down into different components (Figure S5 in Supporting Information S1), the change in MCDD also behaves relatively similarly to NDD. The response to uniform SST warming generally shows an increase in MCDD over tropical and subtropical land (though with substantial regional and inter-model variations), and a decrease over higher northern latitudes. Patterned SST warming causes strong, regionally diverse changes that are extremely model dependent. The fast adjustment causes increases in MCDD over a majority of land areas, but with significant regional exceptions such as in the Sahel region of Africa.

## 4. Discussion and Conclusions

It is well established that global warming has a widespread but non-uniform influence on daily precipitation (Allan et al., 2020; Chadwick et al., 2022; Douville & John, 2021; Douville et al., 2021). The water holding capacity of air increases with temperature by about 7% per °C (Douville, Ribes, & Bock, 2022), which leads to increased atmospheric water vapor and more intense precipitation under warmer climate conditions. Yet, the intensification of the global water cycle does not only manifest as more frequent and stronger precipitation extremes (Douville et al., 2021). Global warming also leads to a reduced frequency of light/moderate precipitation (Chadwick et al., 2022) and to an overall increase in NDD (Polade et al., 2014) in the previous-generation CMIP5 models. In good agreement with these results, the CMIP6 models simulate an overall increase in NDD and MCDD over land in response to an abrupt $CO_2$ quadrupling. This widespread meteorological drying is particularly strong in the subtropics, but is also found in some tropical (e.g., Amazonia) and extratropical (northern mid-latitudes) areas.

The proposed decomposition of the daily precipitation response highlights that the CMIP6 ensemble mean response and related inter-model spread is the combination of multiple drivers. Globally averaged over land,

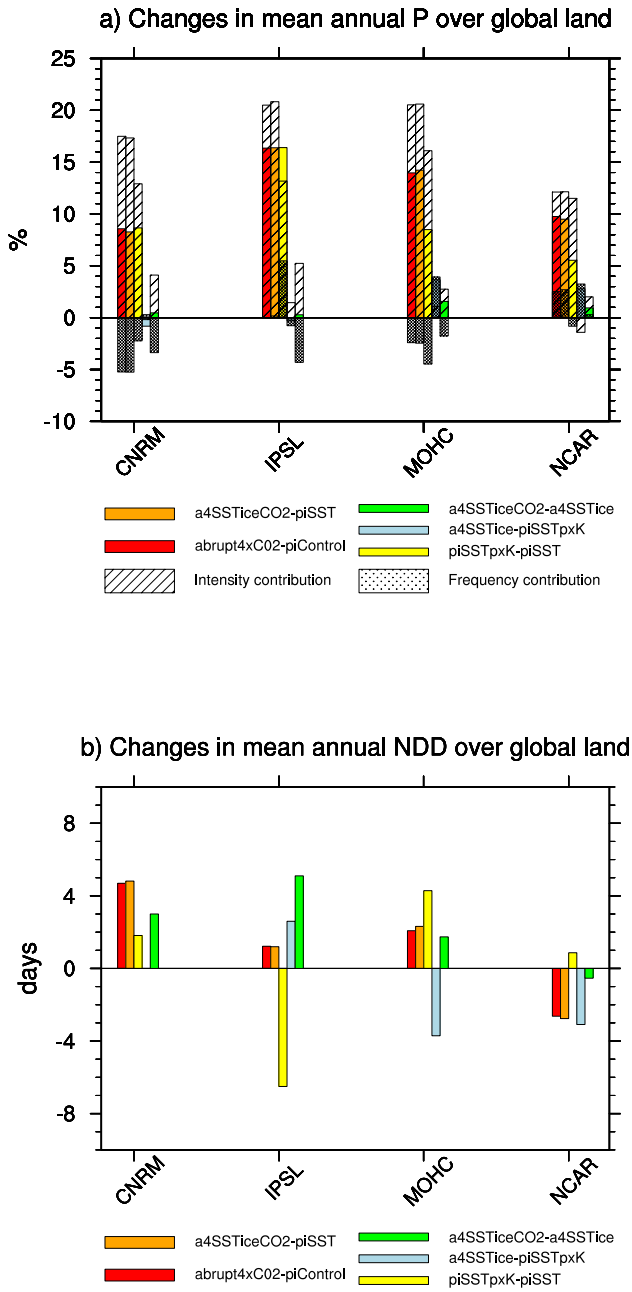


**Figure 4.** Global land aggregated responses and their breakdown into three contributions for (a) relative changes in mean annual precipitation (%) and (b) absolute changes in the mean annual number of dry days. In the top panel, the relative contributions (%) of changes in daily precipitation intensity versus changes in daily precipitation frequency are also shown as dashed and stippled bars, respectively.

the annual mean precipitation increase (Figure 4a) is mostly explained by an increase in daily precipitation intensity (also true for the whole set of CMIP6 models, c.f. Figure S6 in Supporting Information S1) although partly offset by a decrease in daily precipitation frequency in two out of four models. This counter effect arises from both the fast vegetation adjustment to increased $CO_2$ (c.f. Figure S3 in Supporting Information S1) and the uniform SST warming. The land-averaged NDD response (Figure 4b) is even more model-dependent and is not consistently dominated by any specific driver. It should be noticed that our four CMIP6 models are in the upper range of equilibrium climate sensitivity (i.e., above 4.5°C for a $CO_2$ doubling). The model-dependent response to the uniform SST warming is therefore not explained by contrasted global warming levels. The significant contribution of the model-dependent patterns in the SST anomalies (in two out of the four models) and of the fast adjustment to $CO_2$ quadrupling (in three out of the four models) also contribute to a poor scaling of NDD changes with global warming across the model ensemble. This result is also valid at the regional scale (c.f. Figure 3) and is consistent with a previous study highlighting that moisture convergence is poorly constrained by global warming across both CMIP5 and CMIP6 models (Elbaum et al., 2022).

Moreover, the reported drivers of total NDD changes distinguished in Figures 3 and 4b do not tell the whole story about the underlying physical mechanisms. For instance, the fast vegetation adjustment (mostly a stomatal closure effect) is not simply driven by differences in evapotranspiration and recycling rate, but also involves region-dependent processes in which the related land-surface warming interacts with the large-scale atmospheric circulation (e.g., Saint-Lu et al., 2019). Similarly, the fast radiative adjustment involves both regional and remote processes given the associated changes in atmospheric circulation, especially in monsoon regions (e.g., Chadwick et al., 2017; Douville & John, 2021; Mutton et al., 2022). The SST pattern effect also involves changes in large-scale circulation, especially in the tropics where deep convection and associated overturning circulations (Hadley and Walker cells) are sensitive to SST anomalies. The importance of changes in atmospheric circulation can be also diagnosed from a dry static energy (DSE) budget showing that daily precipitation anomalies are not free to respond only to local changes but are also constrained by the horizontal vertically integrated DSE transport (Chadwick et al., 2022).

Beyond the key role of atmospheric circulation, changes in dry day frequency are partly governed by, or at least associated with, local changes in near-surface relative humidity (e.g., Chadwick et al., 2022; Douville & John, 2021), which can regulate the convective inhibition over land (Chen et al., 2020). Such changes are particularly important in the boreal summer midlatitudes, where a near-surface drying is expected (Byrne & O'Gorman, 2016; Chadwick et al., 2016) but could be underestimated by most CMIP5 (Douville & Plazzotta, 2017) and CMIP6 (Douville & Willett, 2023) models. This near-surface drying is the result of a complex interplay between fast adjustments and slower SST-mediated responses, and between both atmospheric and land surface processes (Douville et al., 2020). This strong relationship is also clear in most subtropical areas where the increase in NDD is strongly correlated with a decrease in near-surface relative humidity across the CMIP6 models (Figure S7 in Supporting Information S1). It is, however, a two-way interaction since the lack of precipitation can further increase the near-surface drying, potentially leading to a powerful positive feedback where this ocean-driven drying (Byrne & O'Gorman, 2016) is further amplified by convective inhibition and a growing NDD.

A wider participation in these CFMIP Tier2 experiments would have been useful to check the robustness of our results. Additional process-oriented diagnostics (e.g., DSE budget, convective inhibition and convective available

potential energy) are also needed to assess the proposed physical mechanisms. Better understanding changes in NDD may also contribute to improved projections of precipitation seasonality and interannual variability (Douville & John, 2021; Douville et al., 2021). The so-called "hydrological sensitivity" (Fläschner et al., 2016; Pendergrass, 2020) does not reflect the complexity of the water cycle response to global warming. This number (2.1%–3.1%/K) is relatively robust across the CMIP6 models, but hides a large variety of model behavior regarding the regional and frequency distribution of the daily precipitation rates at which the impacts of water cycle changes are mostly felt. There is therefore a need to look for other metrics (e.g., Giorgi et al., 2011) to better summarize or characterize the overall intensification of the global water cycle.

Finally, we believe the idealized abrupt-4x$CO_2$ experiments may also have practical implications for both mitigation and adaptation strategies given the increasingly dominant effect of $CO_2$ and other well-mixed greenhouse gases on future climate. The emphasized increase in the number of (consecutive) dry days is indeed consistent with the projected increase in meteorological droughts which was assessed by the latest IPCC report (Douville et al., 2021; Seneviratne et al., 2021). Moreover, the distinction between the fast adjustment to increased $CO_2$ versus the slower response to SST changes is also policy-relevant if there is a drastic reduction in atmospheric $CO_2$ due to a large-scale deployment of carbon dioxide removal techniques, and/or a decision to implement solar radiation modification techniques that would mitigate global warming (but not the whole response of dry days) without decreasing the atmospheric $CO_2$ level. This remark again raises caution about the use of global warming levels only to assess climate change and advocate for observational constraints on regional hydrological projections that are not only based on the historical global warming record (Douville, Allan, et al., 2022).

## Data Availability Statement

All model outputs from the CMIP6 DECK and the standard CFMIP experiments are freely accessible at https://pcmdi.llnl.gov/CMIP6/ or at https://esgf-node.llnl.gov/projects/esgf-llnl/. All graphics have been produced using the NCAR NCL software freely accessible at https://www.ncl.ucar.edu/.

**Acknowledgments**
The authors are grateful for the insightful comments from the editor and two anonymous reviewers that help improve the paper greatly. Thanks are also due to all CMIP6 and CFMIP participants, as well as to NCAR for the free access to the NCL software. BM acknowledges support by the U.S. Department of Energy under Award DE-SC0022070 and National Science Foundation (NSF) IA 1947282; the National Center for Atmospheric Research is a major facility sponsored by the NSF under Cooperative Agreement 1852977.

## References

Allan, R. P., Barlow, M., Byrne, M. P., Cherchi, A., Douville, H., Fowler, H. J., et al. (2020). Advances in understanding large-scale responses of the water cycle to climate change. *Annals of the New York Academy of Sciences*, *1472*, 1–27. https://doi.org/10.1111/nyas.14337

Boucher, O., Servonnat, J., Albright, A. L., Aumont, O., Balkanski, Y., Bastrikov, V., et al. (2020). Presentation and evaluation of the IPSL-CM6A-LR climate model. *Journal of Advances in Modeling Earth Systems*, *12*(7), e2019MS002010. https://doi.org/10.1029/2019MS002010

Byrne, M. P., & O'Gorman, P. A. (2016). Understanding decreases in land relative humidity with global warming: Conceptual model and GCM simulations. *Journal of Climate*, *29*(24), 9045–9061. https://doi.org/10.1175/jcli-d-16-0351.1

Chadwick, R., Douville, H., & Skinner, C. B. (2017). Timeslice experiments for understanding regional climate projections: Applications to the tropical hydrological cycle and European winter circulation. *Climate Dynamics*, *49*(9–10), 3011–3029. https://doi.org/10.1007/s00382-016-3488-6

Chadwick, R., Good, P., & Willett, K. M. (2016). A simple moisture advection model of specific humidity change over land in response to SST warming. *Journal of Climate*, *29*(21), 7613–7632. https://doi.org/10.1175/jcli-d-16-0241.1

Chadwick, R., Pendergrass, A. G., Muniz Alves, L., & Moise, A. (2022). How do regional distributions of daily precipitation change under warming? *Journal of Climate*, *35*(11), 3243–3260. https://doi.org/10.1175/jcli-d-20-0864.1

Chen, J., Dai, A., Zhang, Y., & Rasmussen, K. L. (2020). Changes in convective available potential energy and convective inhibition under global warming. *Journal of Climate*, *33*(6), 2025–2050. https://doi.org/10.1175/jcli-d-190461.1

Danabasoglu, G., Lamarque, J.-F., Bacmeister, J., Bailey, D. A., DuVivier, A. K., Edwards, J., et al. (2020). The Community Earth System model version 2 (CESM2). *Journal of Advances in Modeling Earth Systems*, *12*, e2019MS001916. https://doi.org/10.1029/2019MS001916

Donat, M. G., Angélil, O., & Ukkola, A. M. (2019). Intensification of precipitation extremes in the world's humid and water-limited regions. *Environmental Research Letters*, *14*(6), 065003. https://doi.org/10.1088/1748-9326/ab1c8e

Douville, H., Allan, R. P., Arias, P. A., Betts, R. A., Caretta, M. A., Cherchi, A., et al. (2022). Water remains a blind spot in climate change policies. *PLOS Water*, *1*(12), e0000058. https://doi.org/10.1371/journal.pwat.0000058

Douville, H., Decharme, B., Delire, C., Colin, J., Joetzjer, E., Roehrig, R., et al. (2020). Drivers of the enhanced decline of land near-surface relative humidity to abrupt 4x$CO_2$ in CNRM-CM6-1. *Climate Dynamics*, *55*(5–6), 1613–1629. https://doi.org/10.1007/s00382-020-05351-x

Douville, H., & John, A. (2021). Fast adjustment versus slow SST-mediated response of daily precipitation statistics to abrupt-4x$CO_2$. *Climate Dynamics*, *56*(3–4), 1083–1104. https://doi.org/10.1007/s00382-020-05522-w

Douville, H., & Plazzotta, M. (2017). Midlatitude summer drying: An underestimated threat in CMIP5 models? *Geophysical Research Letters*, *44*(19), 9967–9975. https://doi.org/10.1002/2017GL075353

Douville, H., Raghavan, K., Renwick, J., Allan, R. P., Arias, P. A., Barlow, M., et al. (2021). Water cycle changes. In V. Masson-Delmotte, P. Zhai, A. Pirani, S. L. Connors, C. Péan, S. Berger, et al. (Eds.), *Climate change 2021: The physical science basis. Contribution of working group I to the sixth assessment report of the intergovernmental panel on climate change* (pp. 1055–1210). Cambridge University Press. https://doi.org/10.1017/9781009157896.010

Douville, H., Ribes, A., & Bock, O. (2022). Global warming at near-constant relative humidity further supported by recent in situ observations. *Communications Earth & Environment*, *3*(1), 237. https://doi.org/10.1038/s43247-022-00561-z

Douville, H., & Willett, K. (2023). A drier than expected future, supported by near-surface relative humidity observations. *Science Advances*. https://doi.org/10.1126/sciadv.ade6253

Elbaum, E., Garfinkel, C. I., Adam, O., Morin, E., Rostkier-Edelstein, D., & Dayan, U. (2022). Uncertainty in projected changes in precipitation minus evaporation: Dominant role of dynamic circulation changes and weak role for thermodynamic changes. *Geophysical Research Letters*, *49*(12), e2022GL097725. https://doi.org/10.1029/2022GL097725

Fläschner, D., Mauritsen, T., & Stevens, B. (2016). Understanding the intermodel spread in global-mean hydrological sensitivity. *Journal of Climate*, *29*(2), 801–817. https://doi.org/10.1175/JCLI-D-15-0351.1

Giorgi, F., Im, E. S., Coppola, E., Diffenbaugh, N. S., Gao, X. J., Mariotti, L., & Shi, Y. (2011). Higher hydroclimatic intensity with global warming. *Journal of Climate*, *24*(20), 5309–5324. https://doi.org/10.1175/2011JCLI3979.1

John, A., Douville, H., Ribes, A., & Yiou, P. (2022). Quantifying CMIP6 model uncertainties in extreme precipitation projections. *Weather and Climate Extremes*, *36*, 100435. https://doi.org/10.1016/j.wace.2022.100435

Lehner, F., Deser, C., Maher, N., Marotzke, J., Fischer, E., Brunner, L., et al. (2020). Partitioning climate projection uncertainty with multiple large ensembles and CMIP5/6. *Earth System Dynamics*. https://doi.org/10.5194/esd-2019-93

Mutton, H., Chadwick, R., Collins, M., Lambert, F. H., Geen, R., Todd, A., & Taylor, C. M. (2022). The impact of the direct radiative effect of increased $CO_2$ on the west African monsoon. *Journal of Climate*, *35*(8), 2441–2458. https://doi.org/10.1175/JCLI-D-21-0340.1

Pendergrass, A. G. (2020). The global-mean precipitation response to $CO_2$-induced warming in CMIP6 models. *Geophysical Research Letters*, *47*(17), e2020GL089964. https://doi.org/10.1029/2020GL089964

Polade, S. D., Gershunov, A., Cayan, D. R., Dettinger, M. D., & Pierce, D. W. (2017). Precipitation in a warming world: Assessing projected hydro-climate changes in California and other Mediterranean climate regions. *Scientific Reports*, *7*(1), 10783. https://doi.org/10.1038/s41598-017-11285-y

Polade, S. D., Pierce, D. W., Cayan, D. R., Gershunov, A., & Dettinger, M. D. (2014). The key role of dry days in changing regional climate and precipitation regimes. *Scientific Reports*, *4*, 1–8. https://doi.org/10.1038/srep04364

Richardson, T. B., Forster, P. M., Andrews, T., Boucher, O., Faluvegi, G., Fläschner, D., et al. (2018). Carbon dioxide physiological forcing dominates projected eastern Amazonian drying. *Geophysical Research Letters*, *45*(6), 2815–2825. https://doi.org/10.1002/2017GL076520

Saint-Lu, M., Chadwick, R., Lambert, F. H., & Collins, M. (2019). Surface warming and atmospheric circulation dominate rainfall changes over tropical rainforests under global warming. *Geophysical Research Letters*, *46*(22), 13410–13419. https://doi.org/10.1029/2019GL085295

Seneviratne, S. I., Zhang, X., Adnan, M., Badi, W., Dereczynski, C., Di Luca, A., et al. (2021). Weather and climate extreme events in a changing climate. In V. Masson-Delmotte, P. Zhai, A. Pirani, S. L. Connors, C. Péan, S. Berger, et al. (Eds.), *Climate change 2021: The physical science basis. Contribution of working group I to the sixth assessment report of the intergovernmental panel on climate change* (pp. 1513–1766). Cambridge University Press. https://doi.org/10.1017/9781009157896.013

Sillmann, J., Kharin, V. V., Zhang, X., Zwiers, F. W., & Bronaugh, D. (2013). Climate extremes indices in the CMIP5 multimodel ensemble: Part 1. Model evaluation in the present climate. *Journal of Geophysical Research: Atmospheres*, *118*(4), 1–18. https://doi.org/10.1002/jgrd.50203

Skinner, C. B., Poulsen, C. J., Chadwick, R., Diffenbaugh, N. S., & Fiorella, R. P. (2017). The role of plant $CO_2$ physiological forcing in shaping future daily-scale precipitation. *Journal of Climate*, *30*(7), 2319–2340. https://doi.org/10.1175/JCLI-D-16-0603.1

Thackeray, C. W., DeAngelis, A. M., Hall, A., Swain, D. L., & Qu, X. (2018). On the connection between global hydrologic sensitivity and regional wet extremes. *Geophysical Research Letters*, *45*(20), 11343–11351. https://doi.org/10.1029/2018GL079698

Ukkola, A. M., De Kauwe, M. G., Roderick, M. L., Abramowitz, G., & Pitman, A. J. (2020). Robust future changes in meteorological drought in CMIP6 projections despite uncertainty in precipitation. *Geophysical Research Letters*, *47*(11), e2020GL087820. https://doi.org/10.1029/2020GL087820

Voldoire, A., Saint-Martin, D., Sénési, S., Decharme, B., Alias, A., Chevallier, M., et al. (2019). Evaluation of CMIP6 DECK experiments with CNRM-CM6-1. *Journal of Advances in Modeling Earth Systems*, *11*(7), 2177–2213. https://doi.org/10.1029/2019MS001683

Webb, M. J., Andrews, T., Bodas-Salcedo, A., Bony, S., Bretherton, C. S., Chadwick, R., et al. (2017). The Cloud Feedback Model Intercomparison Project (CFMIP) contribution to CMIP6. *Geoscientific Model Development*, *10*(1), 359–384. https://doi.org/10.5194/gmd-10-359-2017

Wilks, D. S. (2016). The stippling shows statistically significant grid points": How research results are routinely overstated and overinterpreted, and what to do about it? *Bulletin of the American Meteorological Society*, *97*(12), 2263–2273. https://doi.org/10.1175/BAMS-D-15-00267.1

Williams, K. D., Copsey, D., Blockley, E. W., Bodas-Salcedo, A., Calvert, D., Comer, R., et al. (2017). The met office global coupled model 3.0 and 3.1 (GC3.0 and GC3.1) configurations. *Journal of Advances in Modeling Earth Systems*, *10*(2), 357–380. https://doi.org/10.1002/2017MS001115